MDPI

Article

Enhancement of Intrinsic Temperature Reduction for Plasma Surface-Modified Nanoparticle-Doped Low-Density Polyethylene Films

Chenlei Qiu [1], Yiping Qiu [1,2,3,4], Yinjia Zhang [2,3] and Lina Cui [2,3,*]

[1] College of Textile and Clothing, Xinjiang University, Urumqi 830046, China; ypqiu@dhu.edu.cn (Y.Q.)
[2] College of Textiles and Apparel, Quanzhou Normal University, Quanzhou 362000, China
[3] Key Laboratory of Clothing Materials of Universities in Fujian, Quanzhou Normal University, Quanzhou 362000, China
[4] College of Textiles, Donghua University, Shanghai 201620, China
[*] Correspondence: cuilina-cui@163.com

Abstract: The cooling performance of nanoparticle (NP)-doped radiative cooling materials depends on the dispersion of the NPs in the polymer matrix. However, it is a technical challenge to suppress agglomeration of NPs due to their high surface energy, resulting in poor dispersion of the NPs in the polymer matrix. In order to optimize the dispersion of zinc oxide (ZnO) NPs in low-density polyethylene (LDPE), NPs were treated with atmospheric pressure plasmas for 30, 60 and 90 s. The ZnO NPs were dispersed in LDPE using a xylene solution method. The dispersion of the NPs was progressively improved as the plasma-treatment time increased, likely due to the roughened and perhaps also activated NP surfaces by the plasma treatment. This made the transmittances of the films decrease in the solar-radiation band and absorptivity increased monotonically in the high-energy band as the plasma-treatment time increased, while in the mid-infrared band, the films maintained a similar high transmittance to the untreated sample. The differential scanning colorimetry analysis revealed that the crystallinities of the plasma-treated NP-doped samples were similar to those of the untreated sample. The cooling-performance tests showed that the maximum temperature reductions of the films with NP plasma-treated for 0 s, 30 s, 60 s and 90 s were 6.82, 7.90, 9.34 and 10.34 °C, respectively, corresponded to the intrinsic temperature reductions of 7.27, 8.23, 10.54, and 11.40 °C, respectively, when calculated using Cui's Model. The results of the current study show that a simple one-step atmospheric pressure plasma treatment to the ZnO NPs can indeed improve dispersion of the NPs in LDPE and lead to the greatly improved passive-cooling performance of the film.

Keywords: plasma treatment; nanoparticles; dispersion; radiative cooling; solar radiation

1. Introduction

In recent years, radiative-cooling materials, as a type of special energy-saving material, are attracting more and more attention due to global warming and worldwide energy shortages [1–5]. In an outdoor environment, the material does not, or only weakly transmits, visible light, while maintaining a high transmission rate to the mid-infrared, thus allowing the lower energy waves to irradiate from inside out to realize the material's radiative-cooling function. A series of new passive-cooling materials have been developed with the improvement of micro/nanomaterial preparation technology [6–8], such as photonic-structured materials [9], nano-hybrid polymer materials [10], and metamaterials [11]. In fact, polymer-based materials are more suitable for scaling up the production and manufacturing of flexible cooling materials, such as films and textiles, than photonic structural materials or metamaterials. Polymers are considered to have strong IR photon emissions in the IR band due to the strong vibrational excitation of different functional

groups in the polymeric chains [12]. For example, the vibrational frequencies in the carbon-halogenated bond fingerprint region (1330–400 cm^{-1}) correspond to a wavelength range within the atmospheric window. This makes many durable halogenated compounds, or their blends, ideal substrates for outdoor passive cooling [2]. These compounds are also quite suitable for the large-scale production of radiative-cooling fabrics. The transmittance of polyethylene materials in the infrared spectral region is excellent compared to conventional textile fabrics ($T_{IR}\% \approx 100\%$), and the heat absorbed by a few characteristic absorption peaks is almost negligible compared to the heat transmitted in the wavelength range of 0.2–16 μm. The optical properties of this material in the solar spectral range can be regulated by doping NPs with different mass fractions and scales [13,14]. ZnO is a semiconductive material that absorbs electromagnetic waves [15] and its characteristic absorption peaks are in the ultraviolet band. The electrical conductivity, dielectric properties, and photocatalysis of polymers can be greatly enhanced by ZnO-NP doping [16–18]. They can also be used as anti-bacterial additives for functional materials [19]. In addition, silver-doped zinc oxide nanoparticles can affect drug content and release effects [20]. The properties of radiative-cooling materials depend on the dispersion of the NPs in polymers [21]. However, NPs are, in general, easily agglomerated due to their extremely large specific surface area and high surface energy [22], leading to their poor dispersion in polymers [23]. This is also thermodynamically unfavorable due to interactions quantified by the Flory–Huggins interaction parameter and the large molecular length of most of polymers [24]. Physical [25–27] and chemical surface-modification [28–31] methods have been adopted to improve the compatibility of NPs with polymers [32,33]. Plasma treatment can modify the surface of a material by releasing high-energy particles during the treatment process, destroying the original bonds between the NP molecules, and altering the surface-energy state of the NPs, so as to improve the dispersion of the NPs in the material [34]. Much attention has been paid to plasma treatments for improving the dispersion of NPs in polymers. Liu et al. treated TiO$_2$-NPs in aqueous solutions of dispersed conductive PEDOT:PSS by DC plasma with pure He at room temperature and atmospheric pressure, while changing constantly the voltage and pH of the solution, which can effectively suppress TiO$_2$ agglomerates and improve the dispersion and stability of TiO$_2$-NPs [35]. Ramos et al. performed surface modification of hBN-NPs using cold vinyl plasma, which led to the deposition of a plasma-polymerized polyethylene layer on the surface of hBN-NPs. The plasma-treated NPs appeared to form fewer and smaller agglomerates, promoting their dispersion in polymers [36]. Saman et al. treated the surface of Al$_2$O$_3$-NPs by atmospheric-pressure plasma with a maximum applied voltage of 10 kVrms in He gas. The results showed that the surface of the NPs was successfully modified, which improved the dispersion and stability of the NPs in nanofluids [37]. Miller et al. studied plasma-surface modification of Al-NPs by a nanosecond AC pulsed power source in an argon atmosphere. Results showed that the plasma treatment created a rough surface morphology to increase surface contact during the reaction process of Al-NPs [34]. However, most plasma-treatment processes are somewhat complicated and thus may be expensive in many end-uses. Another issue is that in most radiative-cooling material testing, laboratory-made devices are adopted and not much attention has been paid to the volume effect on the cooling performance of these materials. In our previous studies, we proposed an empirical model, Cui's Model, to show an exponential relationship between the temperature reduction and specific volume change in the test [38]. The strength of the Cui's Model is that it allows us to calculate the intrinsic temperature reduction (ITR) for a passive-cooling material as a material property instead of a value heavily dependent on the testing set-up. However, we have never used this concept for any other materials or even the same material modified by different treatments. In order to do so, we wanted to use a simple method to change the dispersion of the same nanoparticle in the same film to see how the ITR changed with the material property change. Therefore, in this study, a one-step and simple atmospheric-pressure plasma technique was adopted to modify the surface of ZnO-NPs for improving their dispersion in polyethylene. The NPs were embedded in LDPE to make

the NP radiative-cooling composite films which were tested for their surface morphology, optical, and thermal properties, and radiative-cooling performance to show if the plasma treatment could have, and if so, by how much, an impact on the NP dispersion and various properties of the films. More importantly, we attempted to show, for the first time, how the ITR changed due to the plasma-enhanced dispersion of NPs in the passive-cooling films in this study.

2. Materials and Methods

2.1. Materials

The ZnO-NPs with an average diameter of 90 nm were purchased from Rhawn Chemical Technology Company (Shanghai, China). We selected this particle size since it has an appropriate size parameter for the shielding of a large portion of higher energy photons and a small fraction of lower energy photons of the Vis light [38]. LDPE with a melt index of 25 g/10 min (CAS 9002-88-4) was provided by Aldrich Chemical Company and xylene solvent (CAS 1330-20-7) was supplied by Shenzhen Xilong Technology Company (Shenzhen, China).

2.2. Plasma Treatment

As shown in Figure 1, ZnO-NPs were put in a glass dish which was placed horizontally under the treatment head of the atmospheric pressure glow discharge plasma machine (Model PSPT-2000C, Nanjing Prospect Electronics Technology Company, Nanjing, China). During the treatment, the plasma-discharge treatment head was 2 cm above the NPs and moved back and forth at a constant speed of 10 cm/s. The ZnO-NPs were treated for 30, 60, and 90 s, respectively, with a voltage of 100 V and a power of 3 W under an ambient temperature of 26 °C and relative humidity (RH) of 60%. The reason that we adopted up to 90 s for plasma treatment was to avoid a prolonged treatment time so as to minimize the cost of the process in a real application. In addition, we used air as the treatment media instead of helium or argon, which can be a lot more expensive.
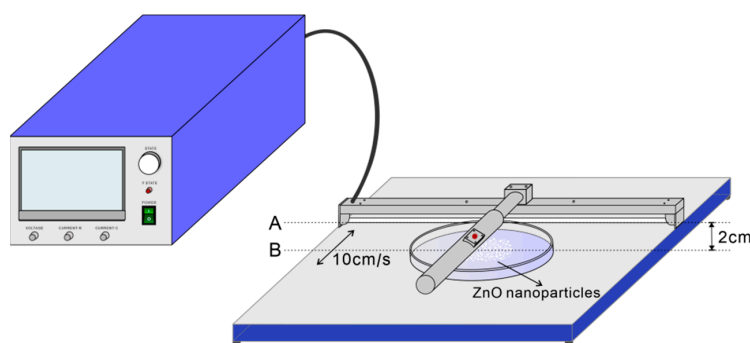

Figure 1. The ZnO NPs were treated by glow discharge plasma equipment.

2.3. Preparation of ZnO-Doped LDPE Films

After the plasma treatment, the ZnO-NPs (4 wt.%) were dissolved in xylene, and subjected to ultrasonic treatment for 60 min in a ultrasonic cell crusher (SCIENTZ-IID, Ningbo, China). The mixture was placed in an oil bath at 105 °C after the addition of LDPE for 48 h. The solvent was then evaporated in a vacuum oven to obtain ZnO/LDPE composites which was hot-pressed at 118 °C to form a film in the vacuum (Shenzhen Jing Ke Da Machinery & Electronic Equipment Company, Shenzhen, China).

2.4. Scanning Electron Microscopy Analysis

The film samples were gold-coated and then inspected with a field emission scanning electron microscope (FESEM, Zeiss MERLIN VP Compact, Oberkochen, Germany) at 5 KV and the chemical elements of the materials were analyzed by EDS energy spectroscopy on the same machine.

2.5. Optical Performance Test

The optical properties of the samples were tested with a Fourier transform infrared (FTIR) spectrometer (Nicolet IS50, Thermo Fisher Scientific, Waltham, MA, USA) and a spectrophotometer (Lambda 950, PerkinElmer, Waltham, MA, USA). Each FTIR spectrum in the wavelength interval of 2.5–16.0 μm was integrated 32 times, while that of 0.2–2.5 μm was integrated 30 times with an interval of 10 nm in order to accumulate enough signal strength.

2.6. Differential Scanning Calorimetry Test

The thermal properties of the ZnO/LDPE films were analyzed with a differential scanning calorimeter (DSC, Model DSC25, TA Instruments, New Castle, DE, USA). The samples were heated from $-80\ ^{\circ}C$ to $180\ ^{\circ}C$ at a rate of $10\ ^{\circ}C/min$ under N_2 conditions, equilibrated for 3 min and then cooled to $-80\ ^{\circ}C$ at a rate of $10\ ^{\circ}C/min$, and continued to be heated to $180\ ^{\circ}C$ at a rate of $10\ ^{\circ}C/min$ after 3 min for a total of 1.5 cycles.

2.7. Radiative-Cooling Performance Test

Passive radiative-cooling tests for the ZnO/LDPE films were conducted using a laboratory-fabricated testing system in Quanzhou, China. The test setup was placed in an outdoor environment on the top of a building throughout the day for 24 h during the summer with daytime temperatures varying in a range of 30–39 °C and RH of about 60%. The test set-up was shown in Figure 2. A temperature sensor was placed 2 cm below the window in the box to monitor and record the temperature change during the test (Figure 2a). The box was made of polystyrene foam, lined with an aluminum foil, and completely sealed to minimize the heat transfer through conduction, convection, and secondary radiation from the outside in and the inside out. The boxes were placed on a desk 1.3 m above the ground to avoid heat transfer from the ground and were able to rotate to face the sun perpendicularly throughout the test. All samples were tested simultaneously to avoid biased sampling. More details of the test system are given elsewhere [38].
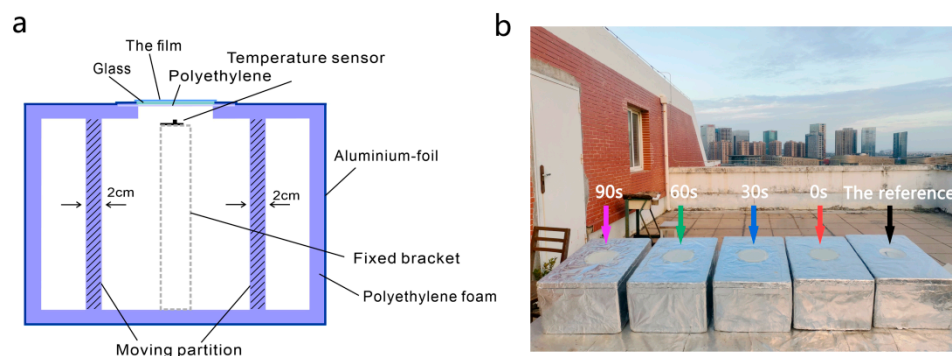

Figure 2. Schematic diagram of the test setup for passive radiative-cooling: (**a**) arrangement inside the passive radiation-cooling test chamber to minimize conduction and convection heat transfer; and (**b**) field experimental setup on the test roof in Quanzhou, China.

2.8. Statistical Analysis

The maximum cooling-temperature data were analyzed using one-way analysis of variance (ANOVA) and Tukey's pair-wise multiple comparison. A *p*-value smaller than 0.05 was considered statistically significant.

3. Results and Discussion

3.1. Morphology Analysis

Figure 3 shows FESEM images of the surfaces of the ZnO-doped LDPE films and distribution of ZnO-NPs on the film surface before and after plasma treatment for different durations. EDS analysis showed that the control sample had the largest number of large particles which are, in fact, the agglomerated NPs. As the plasma-treatment time increased

up to 90 s, more small NPs are shown on the surface of the film, exhibiting better dispersion. Plasma treatment can usually etch the surface of the NPs, especially for atmospheric pressure plasmas. Miller et al. treated Al_2O_3 NPs using atmospheric pressure Ar plasma and found that the NPs were etched by the plasma, resulting in rougher surfaces [34]. In the current study, we observed that the plasma-treated NPs seemed to have better dispersion than the control sample. It is likely that the plasma treatment was able to roughen the surface of the NPs and the surface roughness increased as the plasma-etching time increased up to 90 s. This could result in better dispersion of the NPs in polymers due to reduced agglomeration for NPs with rougher surfaces. FESEM inspection showed that the roughness of NPs surface seemed to increase somewhat after the plasma treatment but was not as visible due to the limited resolution of FESEM at such a high magnification, as shown in Figure 4. The plasma-etching may also have reduced the size of the NPs; however, this effect could not have been significant since the plasma-etching at this power and duration rate may only have removed a couple of nm of the surface layer, as indicated by Miller et al. [34]. We concluded that the plasma treatment is beneficial to the uniform dispersion of ZnO-NPs, and the increased plasma-treatment time will lead to improved dispersion of the NPs in LDPE. The mechanism for the effect of the plasma treatment on NP dispersion in low-density polyethylene (LDPE) may be explained using Figure 5.
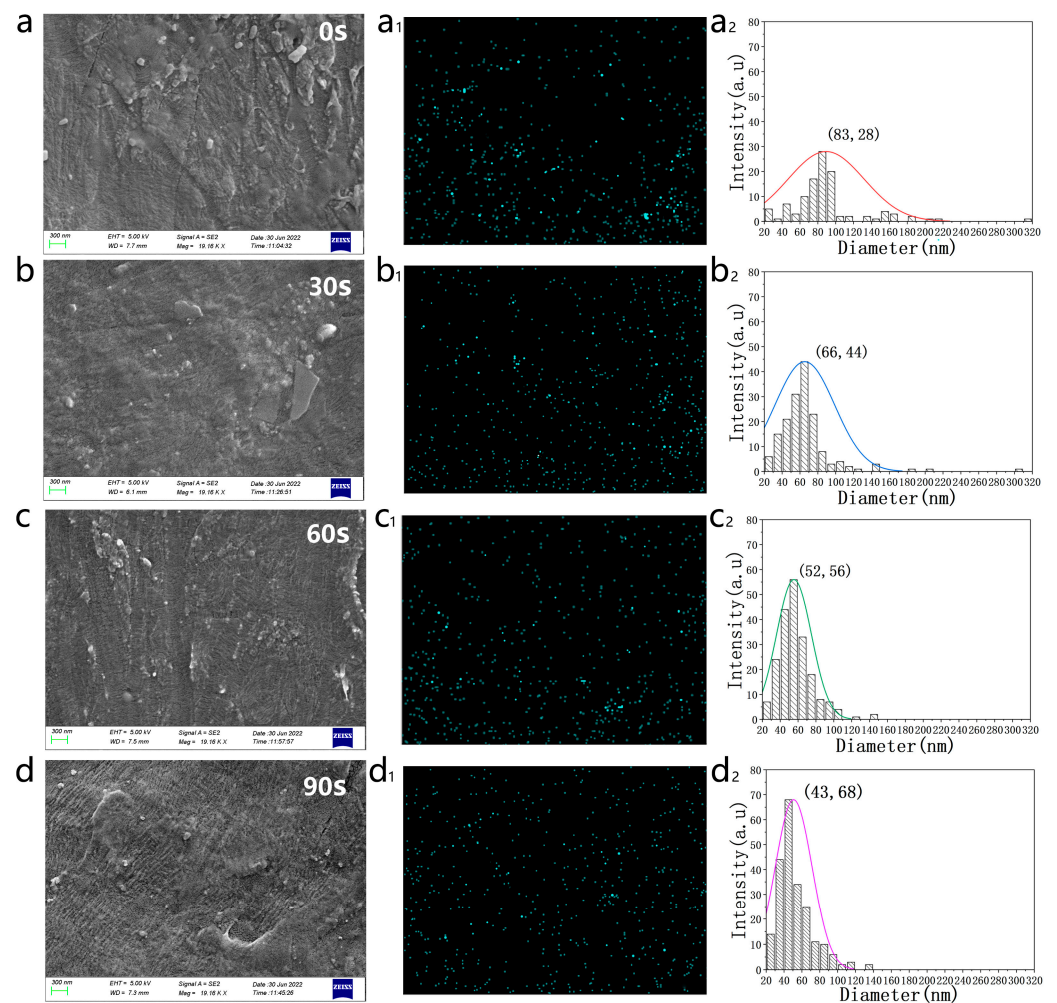

Figure 3. FESEM images of surface morphology and NPs dispersion in ZnO/LDPE films made by plasma-treated NPs: (**a**–**d**) FESEM images of the films made of ZnO treated by plasma for 0 s, 30 s, 60 s, 90 s; (**a₁**–**d₁**) EDS mapping of NPs in films made of ZnO treated by plasma for 0 s, 30 s, 60 s, 90 s; and (**a₂**–**d₂**) particle-size distribution of NPs in films made of ZnO treated by plasma treatment for 0 s, 30 s, 60 s, 90 s.
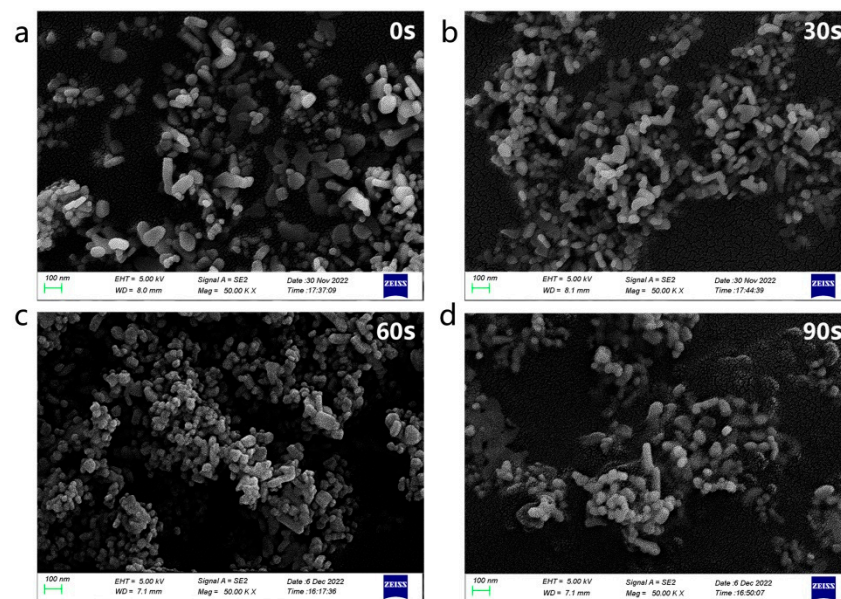
Figure 4. FESEM images of NP surfaces plasma-treated for different durations: (**a**) 0 s; (**b**) 30 s; (**c**) 60 s; and (**d**) 90 s.
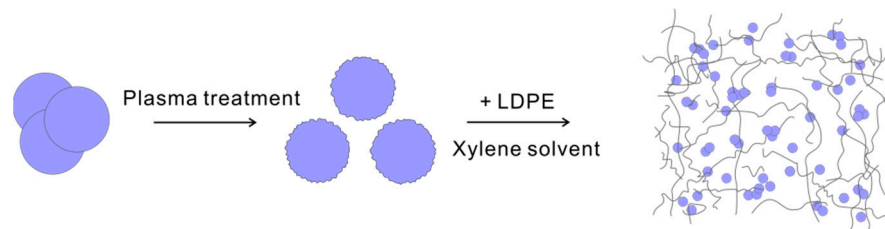

Figure 5. NPs treated by plasma were mixed with LDPE in xylene solvent.

It is possible, as reported in many studies, that plasma can alter the chemical composition of the substrate surfaces such as disrupted surface chemical bonds and implant oxygen containing groups. However, for ZnO-NPs, the development of more oxygen -ontaining groups is unlikely since the NPs are already completely oxidized material. Another approach is to grow organic groups on the surface of the substrate if an organic treatment gas or even pretreatment with organic chemicals could be applied [33]. In future studies, we may try out other treatment processes in order to further improve dispersion of the NPs in LDPE, such as using ethanol pretreatment for growing of methyl or ethyl groups on the surface of the NPs so as to enhance the adhesion between the NPs and LDPE [39].

3.2. Thermal Properties

As shown in Figure 6, DSC endothermic diagrams showed that the crystallinities of the films under different conditions were almost the same, varying by around 37.5%. This means that the plasma treatment had no significant effect on the crystallinity of the films. The crystallization behavior of polymers in the presence of NPs could have been changed if the surface energy of the NPs was altered substantially by the surface treatment of the NPs. It seemed that the surface energy change by the plasma treatment was not significant enough to alter the crystallization behavior of the LDPE film in the current study. The crystallinity of the polymer could influence the radiative-cooling performance of the film. This is because the crystalline phase and the amorphous phase have different refractive indices, which could make the light pass though the material deflected at the boundaries of different phases, greatly influencing the passage of light through the material. A completely amorphous material or a single crystal has the best transparency for all lights. Semicrystalline materials are most likely opaque to most of lights. Therefore, controlling the

crystallinity and size of the crystals in the LDPE could be important for the passive-cooling performance of the materials. Zou and coworkers [40] treated multiwall carbon-nanotubes (MWNTs) with an atmospheric pressure plasma jet with helium and then compounded the MWNTs into polypropylene and polylactic acid resins. They found that the plasma treatment could in fact alter the glass-transition temperature and melting temperature of the composites. The surface of the MWNTs was activated by the plasma treatment, which influenced the adhesion between the MWNTs and the polymers. In the current study, this may not have happened as the substrate was an oxidized material and thus may not have been activated as much as the MWNTs. Therefore, the thermal properties and crystallinity of the films were not altered substantially by the plasma treatment.
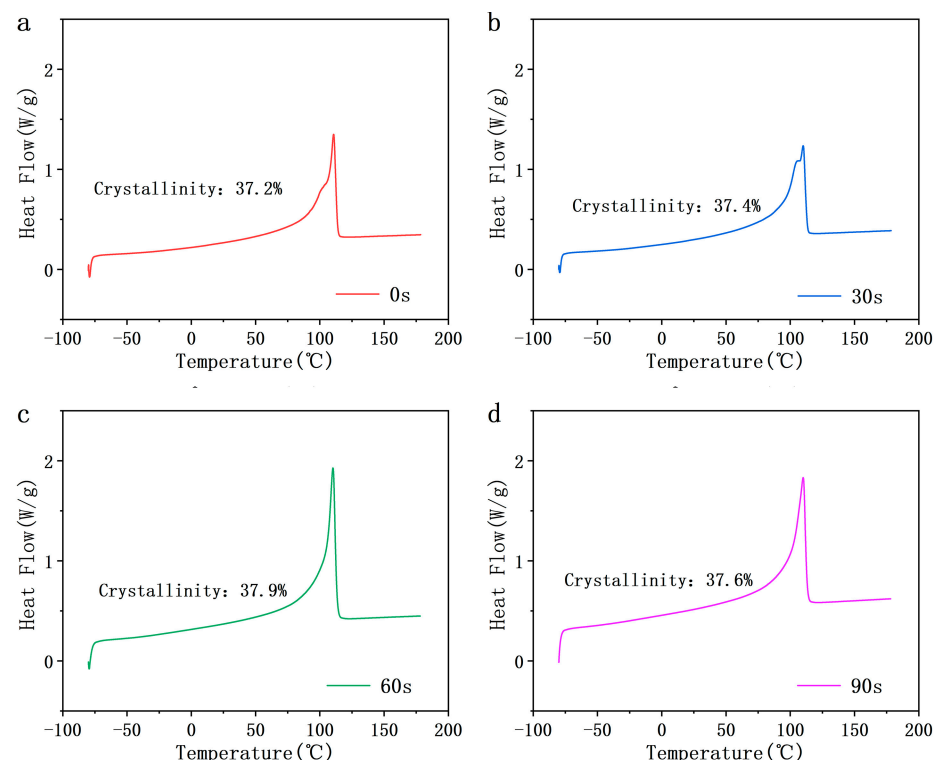

Figure 6. DSC endothermic diagrams of ZnO/LDPE films prepared by different plasma-treatment times: (**a**) 0 s; (**b**) 30 s; (**c**) 60 s; and (**d**) 90 s.

3.3. Transmittance of ZnO/LDPE Films

As shown in Figure 7 and Table 1, the film transmittance shows a declining trend as the plasma treatment time increased due to the enhanced scattering effect of the material on the electromagnetic waves in the visible wavelength band. In Figure 7a, it can be seen from the FTIR spectra that in the high-energy region of visible and near-infrared spectrum, the highest transmittance was obtained for the untreated film and the lowest for the film with NPs plasma-treated for 90 s. In the mid-infrared wavelength range of 2.5–14 μm, all films had similarly good transmittance regardless of the plasma-treatment conditions, indicating that the plasma treatment did not have a significant impact on the transmittance of the mid-infrared range waves. Figure 7b compares the absorptivities of the films made of NPs with different plasma-treatment conditions. Also shown in Table 1, the films tend to have larger absorptivity in the visible wavelength spectrum with the increase of plasma-treatment times. This shows that improved dispersion of the NPs due to the plasma treatment can indeed enhance the scattering effect of the films to the visible light, leading to a reduced transmittance and increased absorptivity in the high-energy irradiation while maintaining the high transmission rate to the mid-infrared waves. This effect corresponds well with the results of the subsequent radiative-cooling performance test.
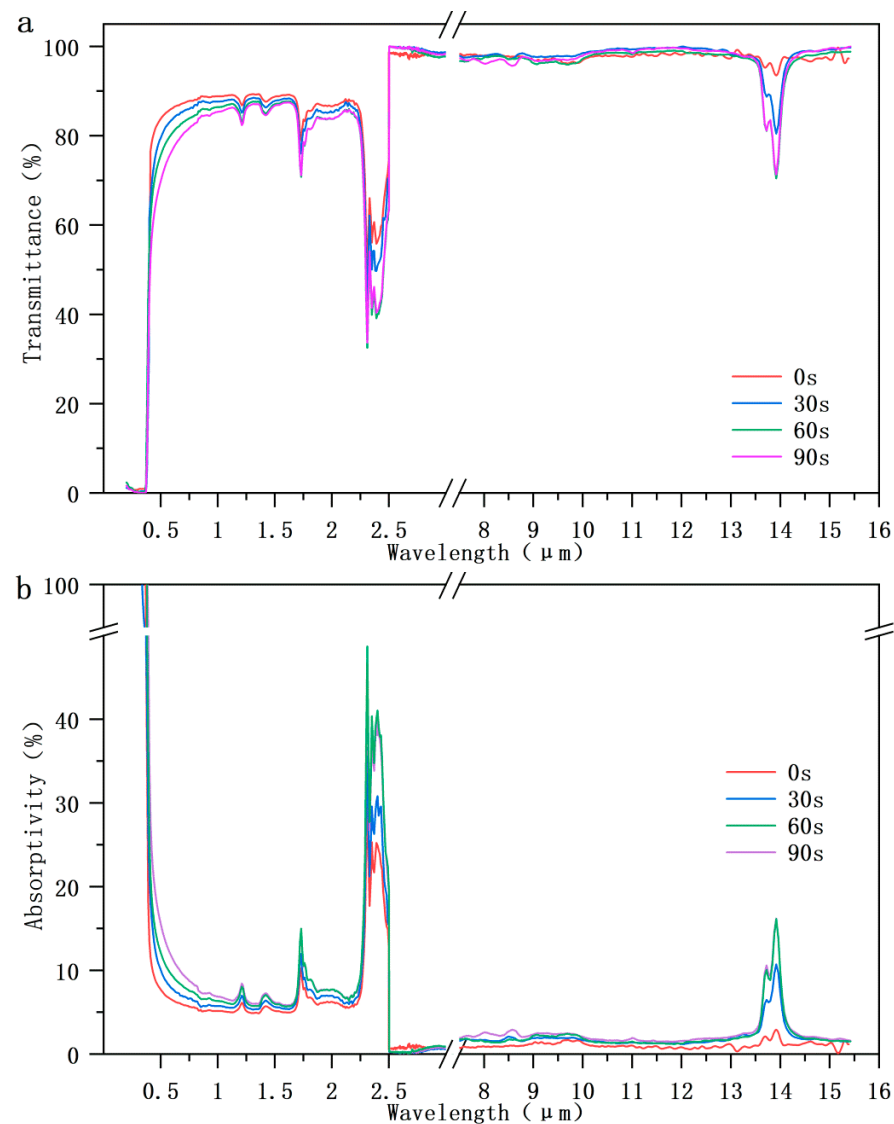
Figure 7. Optical properties of ZnO/LDPE films: (**a**) effect of plasma treatment time on film transmittance; and (**b**) effect of plasma-treatment time on film absorptivity.

Table 1. Transmissivity and absorptivity of the films represented by the area under the FTIR curves.

Area	0 s	30 s	60 s	90 s
Transmissivity curve (s^{-1})	178.1	173.5	168.4	165.9
Absorptivity curve (s^{-1})	0.16	0.19	0.22	0.23

3.4. Cooling Performances

The temperatures of the testing boxes covered with different ZnO/LDPE films were monitored for 24 h to evaluate the films' cooling performance for three days. For reference, a box without a covering film was also tested simultaneously. Overall, the temperature in the reference box rose as the intensity of solar radiation increased, reaching a maximum temperature of 75.41 °C at 12:50, as shown in Figure 8a. The orange area in Figure 8 indicates the daytime solar irradiation, and the films obtained the best cooling performance at 14:20 (AA_1).
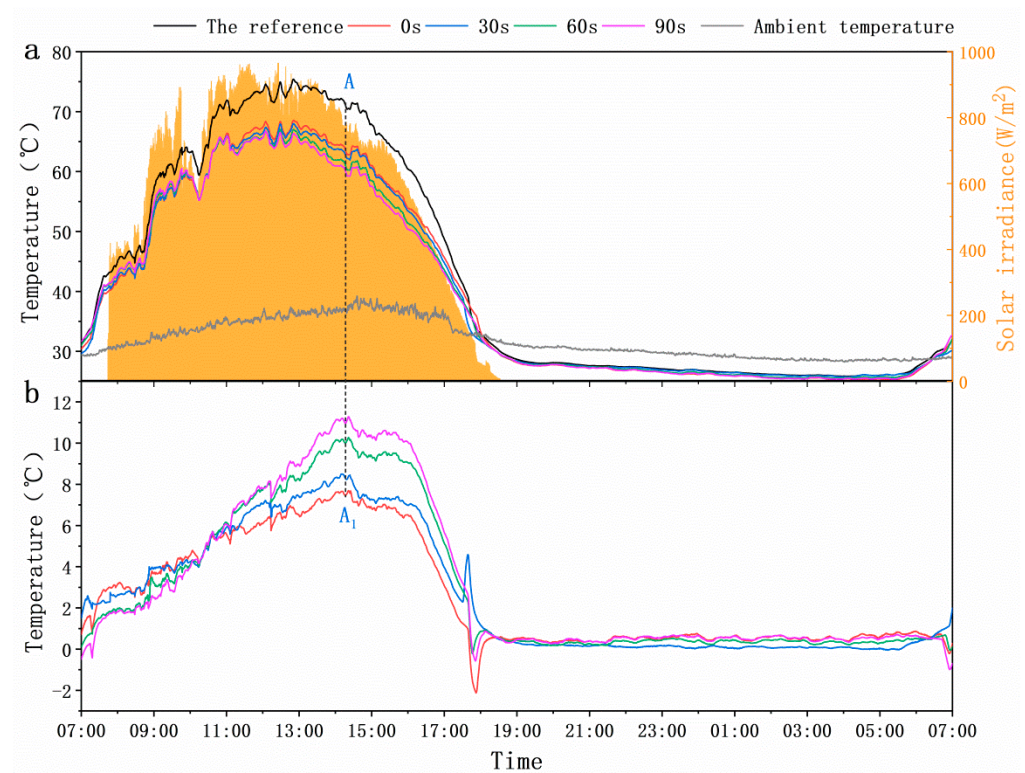
Figure 8. Cooling performance test: (**a**) temperature changes in 24 h in test boxes covered with no film or films prepared by ZnO-NPs with plasma treatment for 0 s, 30 s, 60 s and 90 s; and (**b**) corresponding cooling effect for the boxes with different films.

The maximum temperature reductions of the films with NPs plasma-treated for 0 s, 30 s, 60 s and 90 s were, respectively, 6.82, 7.90, 9.34 and 10.34 °C, indicating a monotonically increasing trend of temperature reduction as the plasma-treatment time increased. The composite film prepared by 90 s plasma treatment of NPs achieved an average cooling value of 10.34 ± 0.72 °C, an improvement of 51.6% compared to the untreated film in Table 2. Meanwhile, the temperatures inside all boxes were lower than the ambient temperature at night, probably due to the shielding effect of the boxes to the heat from the surrounding environment for ambient temperature measurement. This result corresponded well with those from the transmittance tests, in which we found that the films composited with plasma-treated NPs had improved shielding effects for the high-energy radiation as the plasma-treatment time increased but almost no change on the shielding effects of the mid-infrared range waves. In our previous publication [38], we found that the temperature reduction of a radiative-cooling material was a function of the specific volume SV defined as the volume included in the testing box divided by the area of the window covered by the radiative-cooling material. An empirical model, or Cui's Model, was proposed to establish the relation between temperature reduction ΔT and SV as follows:

$$\Delta T = \Delta T_\infty + (\Delta T_0 - \Delta T_\infty)exp\left(-\frac{SV}{D}\right) \tag{1}$$

where ΔT_∞ is the open space temperature reduction as $SV \to \infty$, ΔT_0 is the intrinsic temperature reduction for the film when $SV \to 0$, and D is a constant called cooling effect diminishing constant [38]. According to this model, the ΔT_0 is the material property without the influence of the testing set up. Rearranging Equation (1), we can calculate ΔT_0 as follows:

$$\Delta T_0 = (\Delta T - \Delta T_\infty)exp\left(\frac{SV}{D}\right) + \Delta T_\infty \tag{2}$$

Table 2. Maximum cooling temperature of films prepared by ZnO NPs with plasma treatment for 0, 30, 60 and 90 s.

Specimen	0 s (°C)	30 s (°C)	60 s (°C)	90 s (°C)
1	7.69	8.5	10.27	11.28
2	6.18	7.04	8.58	9.53
3	6.6	8.17	9.17	10.22
Mean ± SD	6.82 ± 0.64	7.90 ± 0.63	9.34 ± 0.7	10.34 ± 0.72
ΔT_0	7.27	8.54	10.23	11.40
Max Improvement (%)	-	17.4	40.6	56.8

In the current study, the experimental set up was the same as that in our previous study and thus we adopted the constant D as 163 m and ΔT_∞ as 4.19 °C while the specific volume in this study was 26 m. The intrinsic temperature reductions, ΔT_0, were calculated using Equation (2) as 7.27, 8.54, 10.23, and 11.40 °C for plasma treatment time of 0, 30, 60, and 90 s, respectively. The improvement from the untreated film were 17.4, 40.6, and 56.8% for the three plasma-treated samples. Figure 9 shows the trend of ΔT_0 versus plasma treatment time, revealing a perfect linear-regression fitted line. This means that the plasma treatment can indeed enhance the radiative-cooling performance of the films and the intrinsic temperature reduction of the films are linearly proportional to the plasma treatment time up to 90 s. This is the first time that any one has been able to show how the surface treatment of NPs could improve intrinsic temperature reduction for radiative0cooling materials as a material property using Cui's Model instead of using temperature reduction directly from the experimental observations, which is heavily reliant on the testing set-up. This made the comparison of materials tested using different experimental set-ups possible.
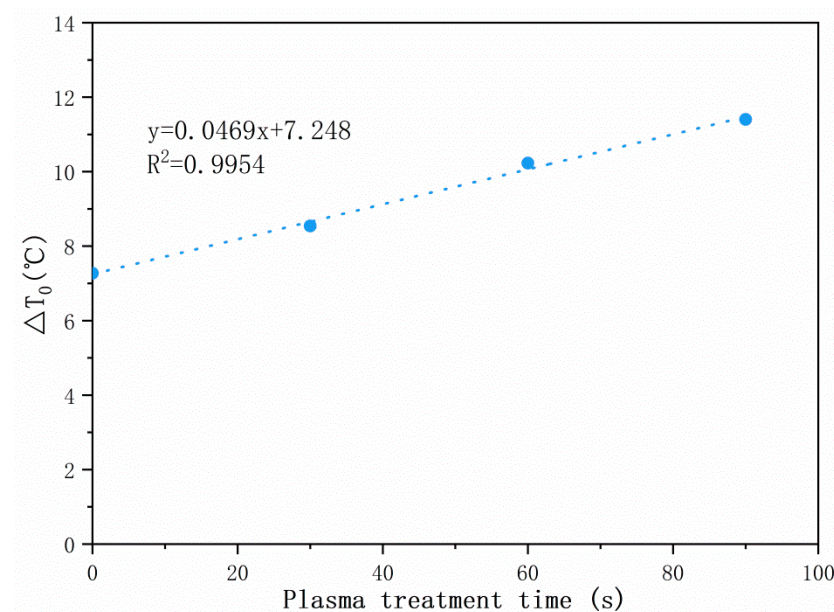
Figure 9. The intrinsic temperature reductions of the passive cooling films as the increase of plasma treatment time, showing a perfect linear -regression fit.

In summary, the ZnO/LDPE film with plasma-treated NPs had better cooling performance because the ZnO-NPs were more uniformly dispersed and the scattering effect was enhanced by the sufficiently long plasma treatment time, shielding the ultraviolet light and blocking most of the light in the visible high-energy region, while the mid-infrared in the 9–14 μm band could be transferred through the radiation window, resulting in the improved cooling effect.

4. Conclusions

ZnO/LDPE transparent films were prepared with ZnO-NPs treated with atmospheric-pressure plasmas for different durations from 30 s to 90 s. It was found that plasma treatment within 90 s effectively suppressed the aggregation of the NPs, making them more uniformly dispersed in the LDPE. The dispersion of ZnO-NPs in LDPE progressively improved as the plasma-treatment time increased from 30 s to 90 s, resulting in enhanced scattering effects. The improved dispersion of the NPs was most likely due to the roughened NP surfaces and activated surfaces by the plasma-etching process. This made the transmittances of the films in the solar-radiation band decrease, and absorptivity increase monotonically in the high-energy band, while in the mid-infrared band, the films kept almost the same high transmittance as the untreated sample. The crystallinities of the untreated and plasma-treated NP-doped LDPE films were almost the same, indicating that the plasma treatment did not change the crystallization behavior of the polymer significantly. The cooling-performance tests showed that the composite film prepared by 90 s plasma treatment of the NPs achieved an average optimal cooling temperature of 10.34 ± 0.72 °C, an improvement of 51.6% compared to the untreated film. The intrinsic temperature reductions, ΔT_0, as calculated using Cui's Model, were 7.27, 8.54, 10.23, and 11.40 °C for plasma-treatment times of 0 s, 30 s, 60 s, and 90 s, respectively. Compared with the untreated film, the improvements were 17.4, 40.6, and 56.8% for the three plasma-treated samples, respectively. A linear increase trend of ΔT_0 as the plasma-treatment time was prolonged was manifested. More studies are warranted to determine how the cooling effect diminishing constant in Cui's model changes for materials with different optical properties.

References

1. Cai, L.; Song, A.Y.; Li, W.; Hsu, P.-C.; Lin, D.; Catrysse, P.B.; Liu, Y.; Peng, Y.; Chen, J.; Wang, H.; et al. Spectrally Selective Nanocomposite Textile for Outdoor Personal Cooling. *Adv. Mater.* **2018**, *30*, 1802152. [CrossRef] [PubMed]
2. Mandal, J.; Fu, Y.; Overvig, A.C.; Jia, M.; Sun, K.; Shi, N.N.; Zhou, H.; Xiao, X.; Yu, N.; Yang, Y. Hierarchically porous polymer coatings for highly efficient passive daytime radiative cooling. *Science* **2018**, *362*, 315–319. [CrossRef]
3. Tong, J.K.; Huang, X.; Boriskina, S.V.; Loomis, J.; Xu, Y.; Chen, G. Infrared-transparent visible-opaque fabrics for wearable personal thermal management. *Acs Photonics* **2015**, *2*, 769–778. [CrossRef]
4. Yang, A.; Cai, L.; Zhang, R.; Wang, J.; Hsu, P.-C.; Wang, H.; Zhou, G.; Xu, J.; Cui, Y. Thermal management in nanofiber-based face mask. *Nano Lett.* **2017**, *17*, 3506–3510. [CrossRef] [PubMed]
5. Cui, L.; Ni, Q.-Q.; Liu, G.; Huang, C.; Zhang, C.; Song, J.; Luo, S.; Qiu, Y. Effect of Nanoparticle Concentration on Passive Cooling Performance of ZNO-Low Density Polyethylene Composite Films Under Solar Radiation. *Sampe J.* **2021**, *57*, 36–45.

6.   Li, W.; Fan, S. Nanophotonic control of thermal radiation for energy applications [Invited]. *Opt. Express* **2018**, *26*, 15995–16021. [CrossRef]

7.   Pereira, J.; Gloria Gomes, M.; Moret Rodrigues, A.; Almeida, M. Thermal, luminous and energy performance of solar control films in single-glazed windows: Use of energy performance criteria to support decision making. *Energy Build.* **2019**, *198*, 431–443. [CrossRef]

8.   Yin, X.; Yang, R.; Tan, G.; Fan, S. Terrestrial radiative cooling: Using the cold universe as a renewable and sustainable energy source. *Science* **2020**, *370*, 786. [CrossRef]

9.   Raman, A.P.; Abou Anoma, M.; Zhu, L.; Rephaeli, E.; Fan, S. Passive radiative cooling below ambient air temperature under direct sunlight. *Nature* **2014**, *515*, 540–544. [CrossRef]

10. Huang, Z.; Ruan, X. Nanoparticle embedded double-layer coating for daytime radiative cooling. *Int. J. Heat Mass Transf.* **2017**, *104*, 890–896. [CrossRef]

11. Zhai, Y.; Ma, Y.; David, S.N.; Zhao, D.; Lou, R.; Tan, G.; Yang, R.; Yin, X. Scalable-manufactured randomized glass-polymer hybrid metamaterial for daytime radiative cooling. *Science* **2017**, *355*, 1062–1066. [CrossRef] [PubMed]

12. Aili, A.; Wei, Z.; Chen, Y.; Zhao, D.; Yang, R.; Yin, X. Selection of polymers with functional groups for daytime radiative cooling. *Mater. Today Phys.* **2019**, *10*, 100127. [CrossRef]

13. Cui, L.; Huang, C.; Xia, H.; Qiu, Y.; Ni, Q.-Q. Transparent ultraviolet-shielding composite films made from dispersing pristine zinc oxide nanoparticles in low-density polyethylene. *Nanotechnol. Rev.* **2020**, *9*, 1368–1380. [CrossRef]

14. Hsieh, A.-H.; Corti, D.S.; Franses, E.I. Rayleigh and Rayleigh-Debye-Gans light scattering intensities and spetroturbidimetry of dispersions of unilamellar vesicles and multilamellar liposomes. *J. Colloid Interface Sci.* **2020**, *578*, 471–483. [CrossRef]

15. Wang, Y.; Gao, X.; Wu, X.; Zhang, W.; Luo, C.; Liu, P. Facile design of 3D hierarchical $NiFe_2O_4$/N-GN/ZnO composite as a high performance electromagnetic wave absorber. *Chem. Eng. J.* **2019**, *375*, 121942. [CrossRef]

16. Ong, T.; Xu, L.; van der Laan, T.A.; Xu, S.; Ostrikov, K. Plasma-aided hydrogenation and Al-doping: Increasing the conductivity and optical transparency of ZnO transparent conducting oxide. *Appl. Surf. Sci.* **2011**, *257*, 9986–9990. [CrossRef]

17. Chen, Z.; Wang, J.; Wu, H.; Yang, J.; Wang, Y.; Zhang, J.; Bao, Q.; Wang, M.; Ma, Z.; Tress, W.; et al. A Transparent Electrode Based on Solution-Processed ZnO for Organic Optoelectronic Devices. *Nat. Commun.* **2022**, *13*, 4387. [CrossRef]

18. Taya, Y.A.; Abd El-Raheem, M.M.; Ali, H.M.; Mohamed, H.A.; Hakeem, A.M.A. Optical and electrical properties of GaZnO films deposited by co-sputtering method on two types of substrates. *Phase Transit.* **2022**, *95*, 581–595. [CrossRef]

19. Mahmoudi Khatir, N.; Abdul-Malek, Z.; Zak, A.K.; Akbari, A.; Sabbagh, F. Sol–gel grown Fe-doped ZnO nanoparticles: Antibacterial and structural behaviors. *J. Sol.-Gel Sci. Technol.* **2015**, *78*, 91–98. [CrossRef]

20. Khatir, N.M.; Sabbagh, F. Green Facile Synthesis of Silver-Doped Zinc Oxide Nanoparticles and Evaluation of Their Effect on Drug Release. *Materials* **2022**, *15*, 5536. [CrossRef]

21. Chandran, S.; Begam, N.; Padmanabhan, V.; Basu, J.K. Confinement enhances dispersion in nanoparticle-polymer blend films. *Nat. Commun.* **2014**, *5*, 3697. [CrossRef] [PubMed]

22. Yuan, W.; Zhou, Y. Reasons for Agglomeration of Nanoparticle and Solutions. *Mater. Rep.* **2008**, *22*, 59–61.

23. LaNasa, J.A.; Neuman, A.; Riggleman, R.A.; Hickey, R.J. Investigating Nanoparticle Organization in Polymer Matrices during Reaction-Induced Phase Transitions and Material Processing. *Acs Appl. Mater. Interfaces* **2021**, *13*, 42104–42113. [CrossRef] [PubMed]

24. Kumar, S.K.; Benicewicz, B.C.; Vaia, R.A.; Winey, K.I. 50th Anniversary Perspective: Are Polymer Nanocomposites Practical for Applications? *Macromolecules* **2017**, *50*, 714–731. [CrossRef]

25. Diao, H.; Si, Y.; Zhu, A.; Ji, L.; Shi, H. Surface modified nano-hydroxyapatite/poly(lactide acid) composite and its osteocyte compatibility. *Mater. Sci. Eng. C* **2012**, *32*, 1796–1801.

26. Shojaeiarani, J.; Bajwa, D.; Holt, G. Sonication amplitude and processing time influence the cellulose nanocrystals morphology and dispersion. *Nanocomposites* **2020**, *6*, 41–46. [CrossRef]

27. Avolio, R.; Gentile, G.; Cocca, M.; Avella, M.; Errico, M.E. Role of silica nanoparticles on network formation and properties in thermoset polycarbonate based nanocomposites. *Polym. Test.* **2017**, *60*, 388–395. [CrossRef]

28. Machrafi, H. On the chemical potential of nanoparticle dispersion. *Phys. Lett. A* **2020**, *384*, 126485. [CrossRef]

29. Mitra, A.; Trifkovic, M.; Ponnurangam, S. Surface Functionalization-Induced Effects on Nanoparticle Dispersion and Associated Changes in the Thermophysical Properties of Polymer Nanocomposites. *Macromolecules* **2021**, *54*, 3962–3971. [CrossRef]

30. Zhang, W.; Lai, E.P.C. Chemical Functionalities of 3-aminopropyltriethoxy-silane for Surface Modification of Metal Oxide Nanoparticles. *Silicon* **2022**, *14*, 6535–6545. [CrossRef]

31. Wang, Y.; Jiang, S. Research progress on surface grafting modification of inorganic nanoparticles based on atom transfer radical polymerization. *New Chem. Mater.* **2019**, *47*, 42–45.

32. Shen, Q.; Xing, D.Y.; Sun, F.; Dong, W.; Zhang, F. Designed water channels and sieving effect for heavy metal removal by a novel silica-poly(ionic liquid) nanoparticles TFN membrane. *J. Membr. Sci.* **2022**, *641*, 119945. [CrossRef]

33. Zendejo-Covarrubias, R.; Idalia Narro-Cespedes, R.; Neira-Velazquez, G.; Cruz-Delgado, V.J.; Ku-Herrera, J.J.; Borjas-Ramos, J.; Arias-Garcia, G.; Soria-Arguello, G. Surface Modification of Graphene Nanoparticles With Ethylene Plasma in Rotary Plasma Reactor for the Preparation of GnP/HDPE Nanocomposites. *IEEE Trans. Plasma Sci.* **2018**, *46*, 2402–2406. [CrossRef]

34. Miller, K.K.; Gottfried, J.L.; Walck, S.D.; Pantoya, M.L.; Wu, C.-C. Plasma surface treatment of aluminum nanoparticles for energetic material applications. *Combust. Flame* **2019**, *206*, 211–213. [CrossRef]

35. Liu, Y.; Sun, D.; Askari, S.; Patel, J.; Macias-Montero, M.; Mitra, S.; Zhang, R.; Lin, W.F.; Mariotti, D.; Maguire, P. Enhanced Dispersion of TiO_2 Nanoparticles in a TiO_2/PEDOT:PSS Hybrid Nanocomposite via Plasma-Liquid Interactions. *Sci. Rep.* **2015**, *5*, 15765. [CrossRef]

36. Borjas-Ramos, J.J.; Ramos-de-Valle, L.F.; Neira-Velazquez, M.G.; Hernandez-Hernandez, E.; Saucedo-Salazar, E.M.; Soria-Arguello, G. Thermal Conductivity of Nanocomposites Based in High Density Polyethylene and Surface Modified Hexagonal Boron Nitride via Cold Ethylene Plasma. *Plasma Chem. Plasma Process.* **2018**, *38*, 429–441. [CrossRef]

37. Saman, N.M.; Zakaria, I.H.; Ahmad, M.H.; Abdul-Malek, Z. Effects of Plasma Treated Alumina Nanoparticles on Breakdown Strength, Partial Discharge Resistance, and Thermophysical Properties of Mineral Oil-Based Nanofluids. *Materials* **2021**, *14*, 3610. [CrossRef]

38. Cui, L.; Huang, C.; Xia, H.; Qiu, Y.; Ni, Q.-Q. Transparent passive-cooling composite films for indoor and outdoor spaces. *Compos. Commun.* **2021**, *24*, 100611. [CrossRef]

39. Jiang, Q.R.; Li, R.X.; Sun, J.; Wang, C.X.; Peng, S.J.; Ji, F.; Yao, L.; Qiu, Y.P. Influence of ethanol pretreatment on effectiveness of atmospheric pressure plasma treatment of polyethylene fibers. *Surf. Coat. Technol.* **2009**, *203*, 1604–1608. [CrossRef]

40. Zou, J.; Zhang, Y.C.; Huang, J.; Wu, H.Y.; Qiu, Y. *Preparation and Properties of PP/PLA/Multiwall Carbon Nanotube Composites Filaments Obtained by Melt Compounding*; Materials Science Forum; Trans Tech Publications: Stafa-Zurich, Switzerland, 2009; pp. 465–468.